Experimental Disparity Analysis of the Behavior and Fatigue of the 304L Stainless Steel

Kada Mouedden, Adel Belattar and Lakhdar Taleb

Abstract This present study investigates the fatigue behavior of the 304L austenitic stainless steel at room temperature. We are particularly interested in the consequences of the experimental disparity on the behavior and on the fatigue of such steel. Thus, several specimens were solicited through the application of symmetrical strain controlled tests with amplitude of 0.22 %. The obtained results show that the evolutions of the stress amplitude of the loaded specimens are almost identical, with a specific fatigue life for each specimen. The evolutions of the isotropic (R) and kinematic (X) parts of the cyclic hardening show that these two components have a similar evolution during the fatigue cycles. The evolution of the discharge slope is similar for all the loaded specimens.

1 Introduction

Due to its superior quality of corrosion resistance, tenacity and ductility, the *304L* austenitic stainless steel is used in many industrial sectors. Several researchers have been interested at its cyclic and fatigue behavior under different types of loading path [1–7] and others.

Cyclic strain controlled tests have been performed under different loading paths. For a proportional low amplitude strain control, the *304L* shows a very limited cyclic hardening (first and second cycle), immediately followed by a cyclic softening [1]. However, under a non proportional load, the metal presents a cyclic hardening; with a slight softening appearing at the end of the cycles.

Therefore, the most powerful cyclic hardening can be obtained for a non proportional loading path, as it significantly increases the hardening period (number of

K. Mouedden (✉) · A. Belattar · L. Taleb
GPM, INSA de Rouen, Normandie Université, CNRS UMR6634,
BP. 8 avenue de l'université, St Etienne du Rouvray, 76800 Rouvray, France
e-mail: kada.mouedden@insa-rouen.fr; kada.mouedden@yahoo.fr

K. Mouedden · A. Belattar
Département des Sciences et Technologie, AMC,
BP 48 Cherchell Terre, 42006 Tipaza, Algeria

cycles), which is very short compared to the proportional loading path. Additionally, a phenomenon called cross-hardening effect has been observed; this phenomenon appears when a proportional cyclic loading at a specific direction is followed by another proportional cyclic loading in a different direction. The cyclic additional hardening is observed immediately after the changing in loading direction, followed by a cyclic softening [1, 8].

The previous work conducted by Belattar [9] were interested in the effects of the cyclic pre-hardening, axial or torsional, on the cyclic behavior and the fatigue lifetime of the *304L* stainless steel. The sequential cyclic test carried out with increasing or decreasing of strain amplitude has confirmed the strain memory effect on the cyclic curve of the *304L*. The study of the isolated effect of the pre-hardening on the fatigue without the intervention of the mean stress was possible through the application of the sequential loading as pre-hardening loading. Compared to the previous researches with a similar objective [6, 10, 11], the application of a sequential pre-hardening assures a progressive return at zero stress-strain at the end of the process of the pre-hardening, which allows us to study the isolated effect of the pre-hardening. The obtained results show that the lifetime was significantly reduced for the pre-hardened specimens compared with the non pre-hardened ones. This lifetime reduction is related to the formation of dense dislocation structures inherited from the pre-hardening phase. Additionally, it was also shown that increasing of the fatigue strain amplitude reduces this pre-hardening effect especially for the torsion pre-hardening case. However, concerning the axial pre-hardening at a low amplitude fatigue strain (0.22 %), obtained results showed that the axial pre-hardening has almost no effect on the fatigue lifetime of the *304L*.

The objective of this present work is to explore these latest results of previous works in order to study the lifetime disparity of the *304L*, especially the fatigue strain amplitude of 0.22 %, by analyzing the contribution of the isotropic and kinematic hardening components of each performed test.

2   Material, Specimen and Experimental Procedure

The material used in this study is an austenitic stainless steel *304L* grade THYSSEN, commercially obtained in the bars form. The chemical composition of this nuance is reported in Table 1 in percentage by weight transmitted by the provider. After machining, the test specimens were heat treated at 1050 °C (in primary vacuum) for 1 h followed by slow cooling to room temperature to obtain a homogeneous mechanical and metallurgical state. This heat treatment also aims to relax the internal stresses introduced during machining.

Table 1 Chemical composition in weight percent of 304L

C	Cr	Ni	Si	Mn	S	P	N_2	Mo	Cu	Fe
0.028	18.5	10	0.68	1.54	0.026	0.035	0.085	/	/	Remain

The mechanical tests were performed on tubular cylindrical specimens with the outer and inner diameters are respectively 20 and 17 mm with a length of 46 mm in gauge section. However, axial displacement and strain measurements were made with an MTS extensometer having 12 mm gage length (distance between the knives of the extensometer), this geometry is more suitable for axial loads in ten-sion-compression. This type of tubular specimens is recommended to perform low cycle fatigue tests where the temperature increase is important. Due to its geometry the cooling is easier. The fatigue tests were performed on a servo-hydraulic MTS machine tension-torsion. It has a singular capacity for control of tension and compression tests ($\pm$250 kN, $\pm$75 mm) or torsion ($\pm$2220 Nm, $\pm$45°). It allows for testing imposed strain or imposed stress.

In order to realize the given objectives, three tension-compression controlled strain fatigue tests were performed with an amplitude of 0.22 % at room temperature with a frequency of 0.1 Hz for the 100 first cycles and 5 Hz during the rest of the cycles, these tests were performed on virgin specimens of nuance *304L* Thyssen.

This study is based on the results of the three fatigue tests, as well as two other tests performed by Belattar [9]. These last two are executed with a frequency of 1 Hz for the first 500 cycles and a frequency of 5 Hz was applied during the remaining cycles. Table 2 includes all tests on *304L-Com* nuance.

We sought through the application of a low frequency (1 Hz) during the first cycles of our tests to present the material behavior at the beginning of life. The results obtained by Kpodekon [10] showed that the frequency change did not have a significant influence on the stress response. This change does not alter the strain mechanisms during the fatigue cycles. During the different fatigue tests, the evolutions of displacement and force are recorded in a file according to time and number of cycles. In order to calculate the axial stress, plastic strain, stress amplitude and other parameters we used different expressions presented in Table 3. Figure 1 shows the main characteristic parameters of a hysteresis loop.

In order to confirm the good progress of these axial fatigue tests, the evolution of torque versus time was controlled for five tests. From Fig. 2a, we find that the torque values remain insignificant, so they are not involved during the fatigue tests.

The fatigue tests were performed in zero mean stress conditions. Figure 2b shows the evolution of the mean stress versus number of cycles for the *Ax1*_0.22 % test, we note that the evolution of the mean stress is not significant during cycles. We can therefore consider that the cyclic test is really performed at zero mean

Table 2 Description of the various tests carried out as part of this study

Nuance	Specimen type	Stress rate (s^{-1})	Reference (%)
304L (nuance THYSSEN)	Specimen tubular (blank)	0.1 Hz for the first hundred cycles; −5 Hz for the rest.	Ax1_0.22 %
			Ax2_0.22 %
			Ax3_0.22 %
		−1 Hz for the first 500 cycles; −5 Hz during the remaining cycles.	Ax4_0.22 % [12]
			Ax5_0.2 % [12]

Table 3 Relationships used to calculate variable analysis obtained from the mechanical tests

Parameters	Formula	Unit
Axial total strain	$\varepsilon = \frac{\Delta l}{l_0}$, $l_0 = 12\,\text{mm}$	unitless
Axial stress	$\sigma_{11} = \frac{F}{S}$, $S = \frac{D_{ext}^2 - D_{int}^2}{4} = 87\,\text{mm}^2$	N/mm^2 (MPa)
Axial plastic deformation	$\varepsilon_{11}^P = \varepsilon_{11} - \frac{\sigma_{11}}{E}$, E : Elastic modulus	unitless
Stress amplitude	$\sigma_a = \frac{\Delta\sigma}{2} = \frac{\sigma_{max} - \sigma_{min}}{2}$	N/mm^2 (MPa)
Mean stress	$\sigma_{moy} = \frac{\sigma_{max} + \sigma_{min}}{2}$	N/mm^2 (MPa)

Fig. 1 The main parameters calculated on a hysteresis loop
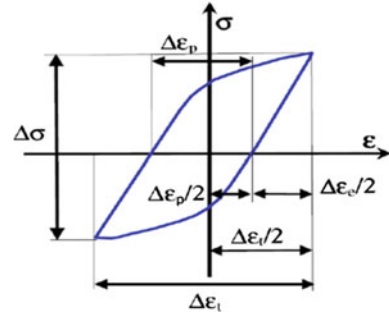
stress. We present only the evolution of the mean stress of this test because the other tests have a similar evolution compared to this one. The tests were performed on virgin specimens (without effect of pre-hardening) at room temperature. This shows that tests are carried without any interference parameter on the fatigue behavior of this steel.

3 Results

In order to clarify the cyclic behavior of the different specimens, we are compared in Fig. 3 the evolutions of stress amplitudes according to the number of cycles. The fatigue life time of the specimens 1–5 are respectively 122099, 133199, 84099, 132099 and 154599 cycles. We note an important difference between these life-times. These results show that there is a disparity of different specimens even if their chemical compositions and mechanical stresses were identical.

Regarding the evolution of the stress amplitude, it is observed that the three curves obtained from tests (*Ax_1 to 3*) are very close. The behavior as a function of number of cycles can be decomposed into three phases. The specimens show a first cyclic hardening phase during the first few cycles. Then a gradual decrease in the rate of consolidation to the maximum stress amplitudes was observed and then a cyclic softening. These observations are reflected in reduced stress amplitude at the
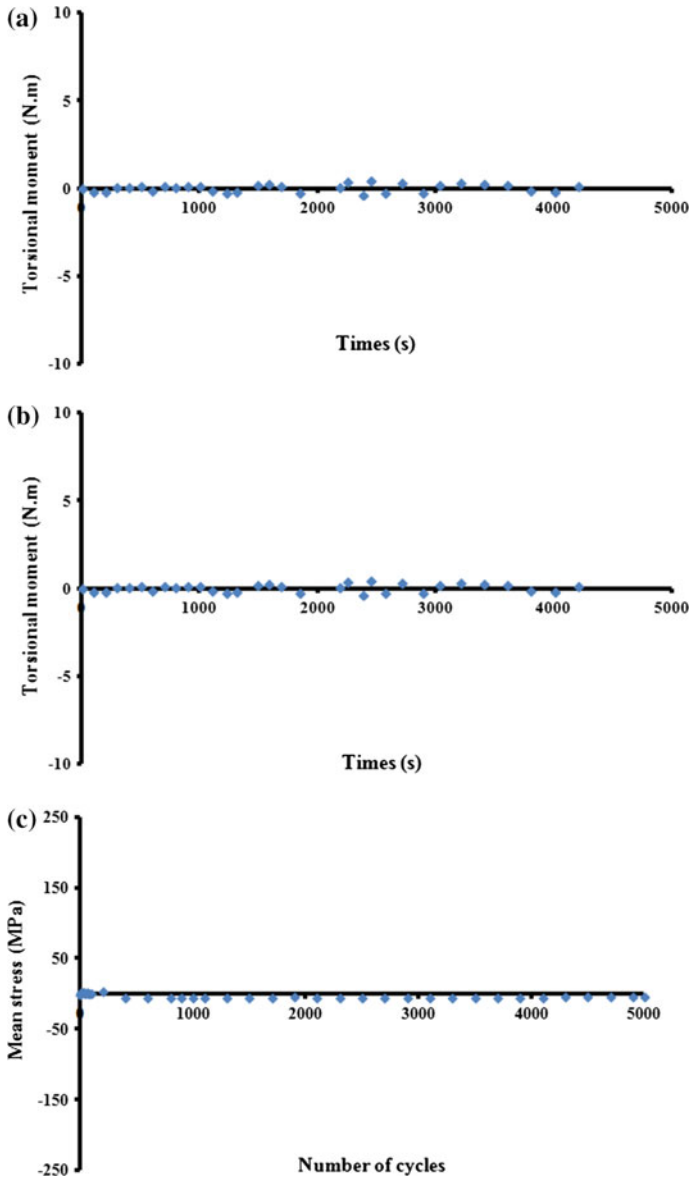
Fig. 2 Evolution of **a** torque as a function of time and **b** the mean stress versus number of cycles for first test

beginning of cyclic loading followed by stabilization from the 1000th cycle. Finally, in the vicinity of the fracture stress amplitude decreases rapidly.

About the two other tests, carried out by Belattar [9, 12], we note that the setpoint has been reached 0.22 % from the 100th cycle. A comparison was made
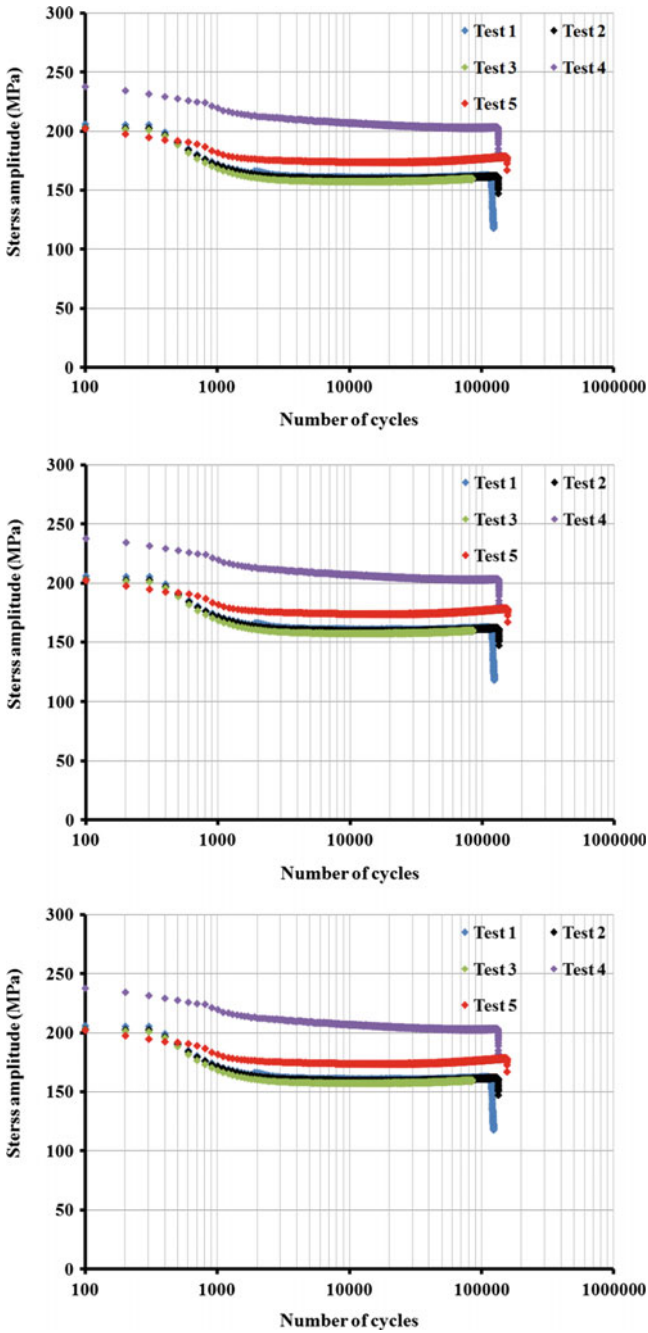
Fig. 3 Evolution of the stress amplitude versus number of cycles for the five fatigue tests

between the evolutions of the amplitude stress for *Ax_4* and *Ax_5* tests, both specimens exhibit a softening until the stabilization of the stress amplitude. We note that from about the 100th cycle, the five specimens have the same qualitative and quantitative representations. However, the fourth specimen has a gap of the order of 40 MPa during the stabilization phase compared to the other samples. The differences between the stresses amplitudes of three specimens tested in this study are not significant, even if their fatigues lifetimes are different.

In order to analyze the cyclic behavior of the material, we present in Fig. 4 the evolution of hysteresis loops at the beginning, mid-life and near to fracture for the
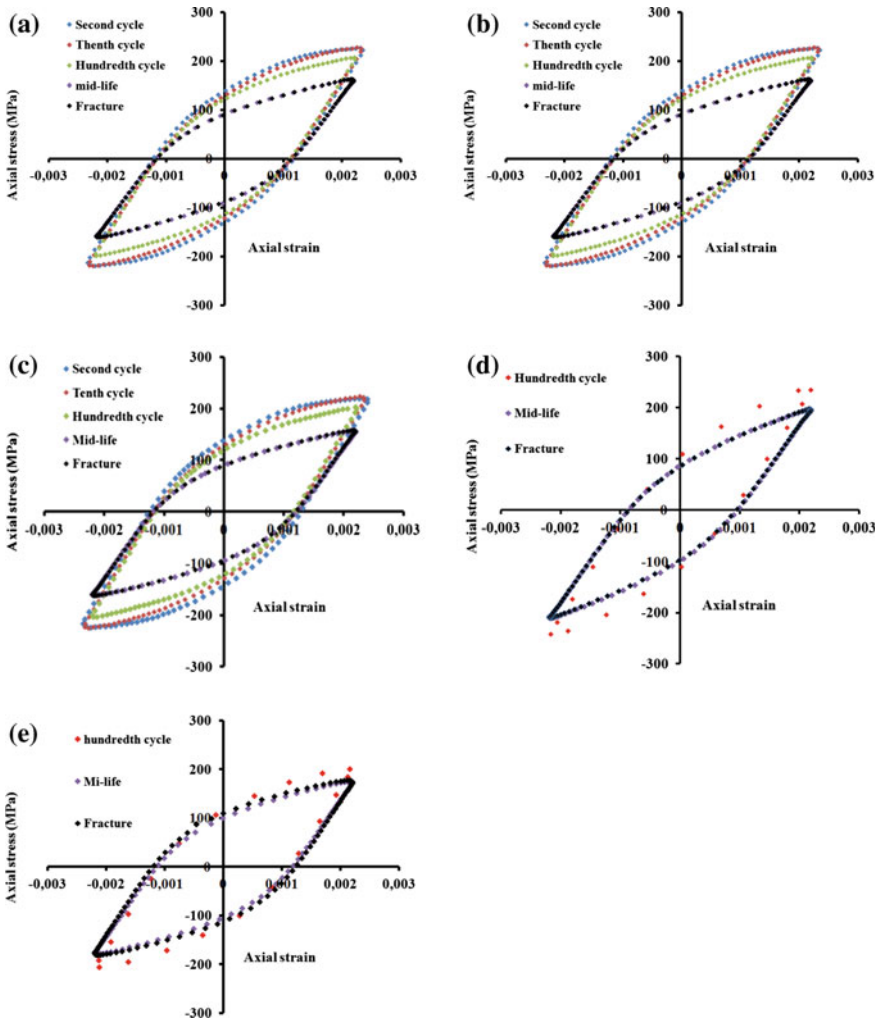

Fig. 4 Evolution and comparisons between hysteresis loops obtained during fatigue testing to 0.22 % **a** Ax_1, **b** Ax_2, **c** Ax_3, **d** Ax_4 and **e** Ax_5

five tested specimens. The observation of Fig. 4 which includes the evolutions axial stresses in function of axial strains, gives the following remarks:

- All loops are perfectly symmetrical attesting to zero mean stress during the tests;
- For *Ax_1*, *Ax_2* and *Ax_3* fatigue tests: we can observe a slight cyclic hardening limited to the first five cycles followed by a progressive cyclic softening up to about 100th cycles. A rapid reduction in axial stress after these cycles is observed which stabilizes until failure;
- Concerning *Ax_4* and *Ax_5* fatigue tests: the hysteresis loops (d) and (e) show that both specimens show a cyclic softening from about 100th cycles. During the stability the hysteresis loops are superposed;
- The plastic strain amplitude is similar to the five tests specimens. However, any gap between the axial stress in particular from the first three specimens and that of Belattar [9, 12] is observed.

The curve of the evolution of maximum stresses as a function of number of cycles confirms the previous observations. From Fig. 5, we notice a decrease of maximum stress between 100 and 1000 cycles followed by stabilization of the maximum stresses phase until it failure. A small gap is found between *Ax_1*, *Ax_2* and *Ax_3* tests; however there is a difference of about 40 MPa between these tests and the fourth. These results highlight the existence of a disparity lifetimes of *304L* grade Thyssen loaded in oligocyclic fatigue in low imposed strain amplitude.

In the following, and in order to explain the recorded observations, we carried out an analysis of the evolution of the kinematic and isotropic cyclic hardening components as well as the elastic modulus. From a macroscopic viewpoint, the evolution of the isotropic hardening represents the variation in the size of the elastic domain. The evolution of *X* shows the evolution of the elastic domain center.
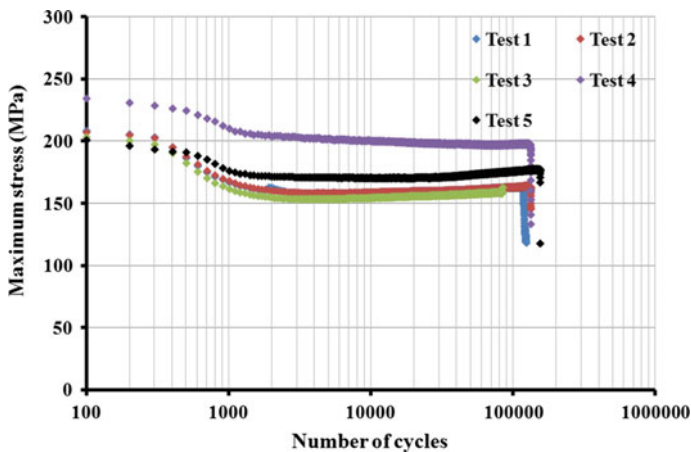

Fig. 5 Evolution of maximum stress as a function of the number of cycles for the five tests

4 Evolution of Cyclic Hardenings

In this section we examine the contribution of the isotropic and kinematic hardening generated during these five fatigue tests. The estimation of parameters for these two types of hardening has been described several times in the literature [13, 14] in tension-compression and in biaxial loading conditions [1]. They are determined from the hysteresis loops generated during the loading cycles, as shown in Fig. 6. Firstly, we identify the maximum stress (σ_{max}). Then, from the point ($\sigma_{max}, \varepsilon_{offset}$) an offset is applied corresponding to a plastic strain of 0.0002, ε_{offset} is the stress associated with this plastic strain. The determination of X and R also involves the identification of the elastic limit σ_y, which is calculated from the first cycle during discharge. It is noteworthy that the evaluation of R and X has been realized by an

Fig. 6 **a** Estimation of isotropic R and kinematic X cyclic hardening in the case of axial loading. **b** Procedure for the identification pseudo elastic modulus [15]
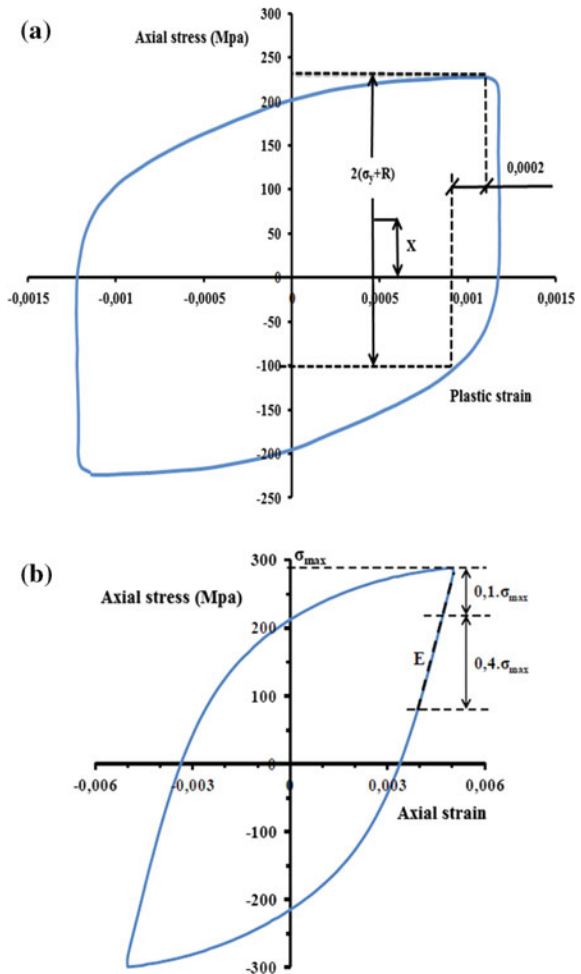
offset of 10^{-4} and 2×10^{-4}. The kinematic (X) and isotropic (R) cyclic hardening are given by the following relationships:

$$R = \frac{\sigma_{max} - \sigma_{offset}}{2} - \sigma_y \quad and \quad X = \frac{\sigma_{max} + \sigma_{offset}}{2} \tag{1}$$

However, this identification process presents some limitations. The selection of offset has a great influence on values of kinematic and isotropic cyclic hardening.

For this purpose, we preferred an identification with both offset (0.0001 and 0.0002). The evolutions of X and R of the five tests for an offset of 2×10^{-4} are presented in Figs. 7 and 8, we preferred to exhibit the evolutions of R and X for specimens 1, 2 and 3 from the first cycles in order to show the behavior during the first 100 cycles.
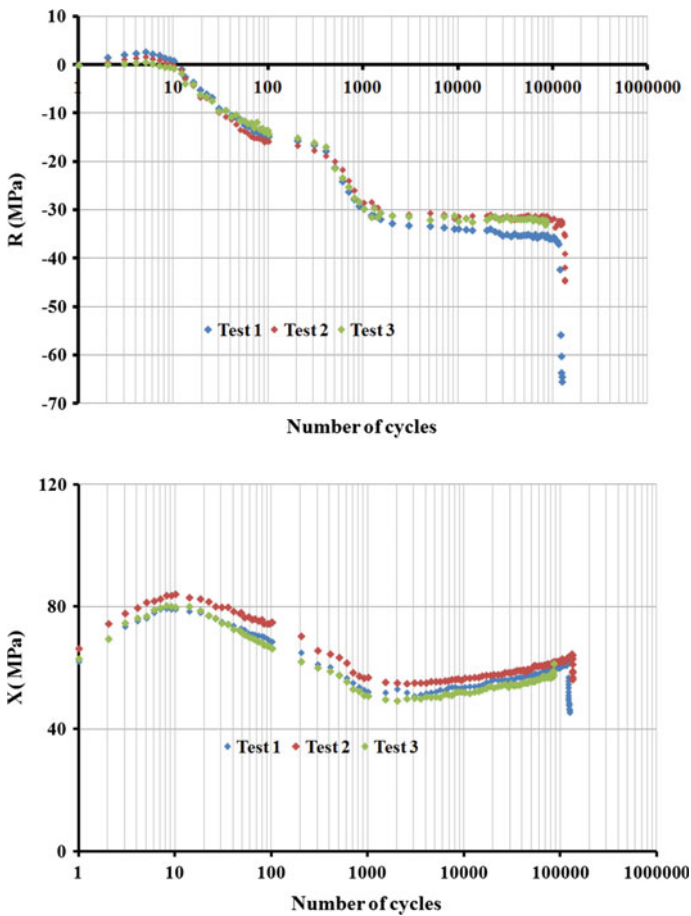

Fig. 7 Comparison between evolutions of R and X (calculated with offset = 0.0002) of first, second and third tests
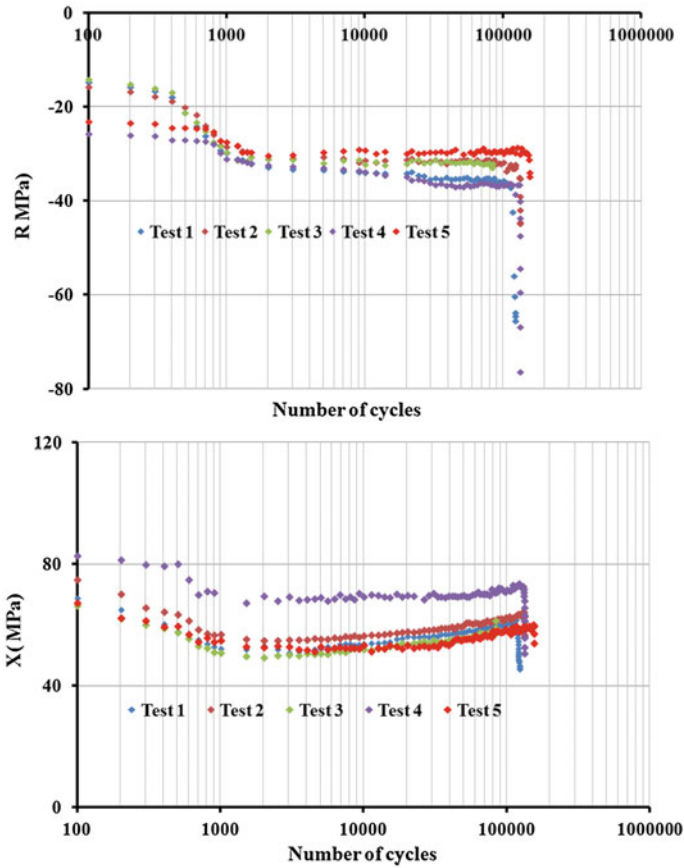
Fig. 8 Comparison between R and X evolutions of the five tests (calculated with offset = 0.0002)

Figures 7, 8, 9 and 10 shows a comparison for evolutions of R and X from the 100th cycles of the five tests. We can do the following findings:

- For the five tests the kinematic hardening is more important than the isotropic hardening;
- The kinematic hardening (X) increases during the first few cycles and then decreases and increases again until failure for the first three tests;
- The kinematic hardening for the fourth and the fifth specimens shows a decrease from the 100th cycles followed by an increase until failure. Nevertheless the evolution of X for the fourth specimen exhibited a small increase after about 1000 cycles;
- From the 100th cycles, the kinematic hardening for the specimens number 1, 2, 3 and 5 is identical, against the specimens number 4 which has a gap about of 10 MPa relative to other specimens;
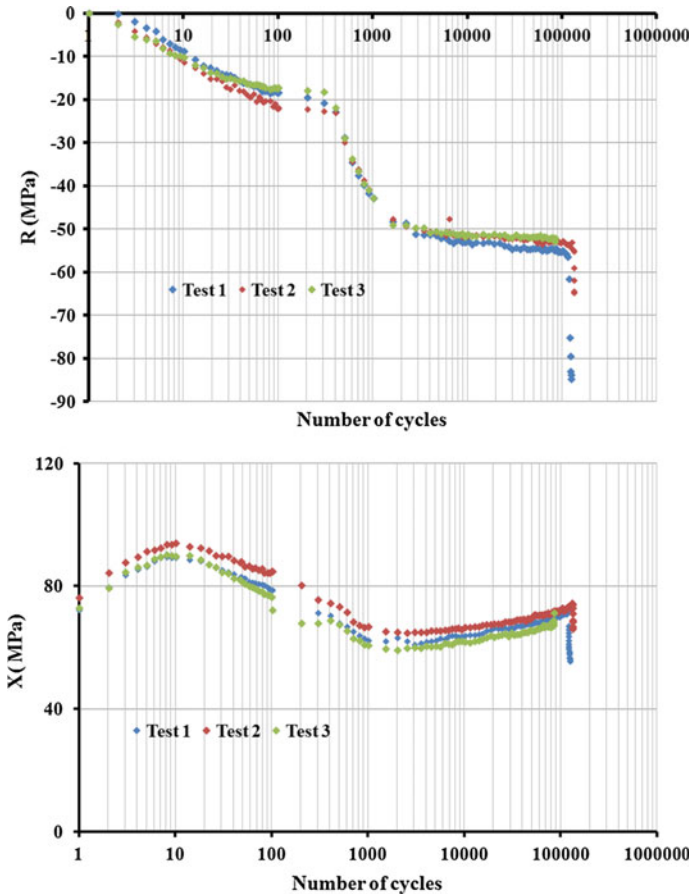
Fig. 9 Comparison between evolutions of R and X (calculated with offset = 0.0001) of first, second and third tests

- The evolution of the isotropic hardening of three first fatigue tests shows that the latter exhibit an increase during the first five cycles which indicates the cyclic hardening observed at the beginning, followed by a decrease for this variable, reflecting the observed cyclic softening. After the 100th cycle a fast decrease of R is observed followed by a phase of stability until failure;

A comparison for R of the five fatigue tests showed that all specimens are similar curves with a small difference, the difference observed between our tests and those of Belattar [12] is of the order of 5 MPa which remains insignificant. Figures 9 and 10 exhibit the evolutions of kinematic and isotropic cyclic hardening estimated with an offset of 0.0001. Figure 9a shows the variation of R as a function of cycles for the first, second and third fatigue tests. We note that this parameter is negative in all cycles which are contrary to the cyclic hardening observed in the first cycles.
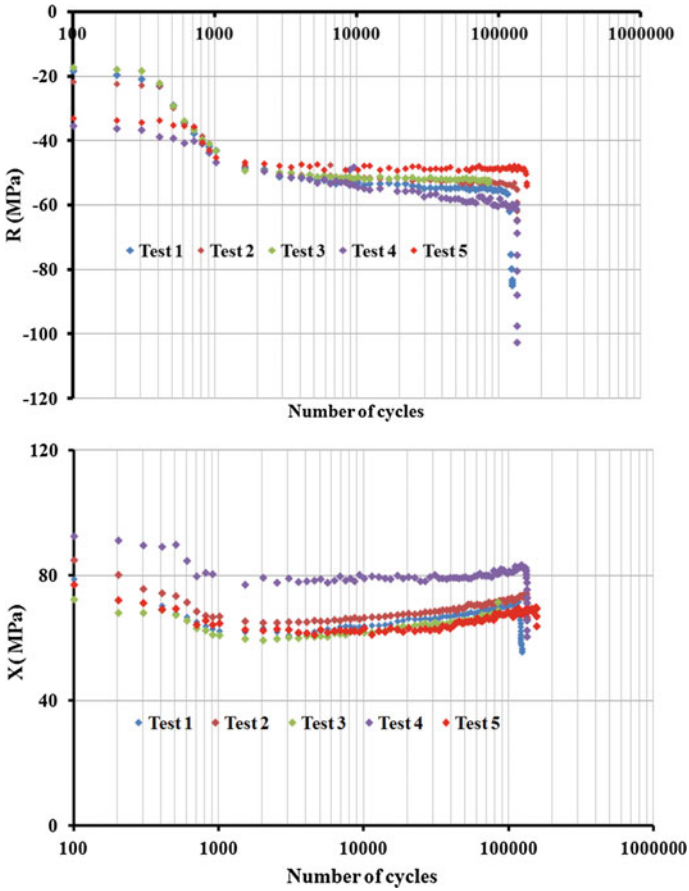
Fig. 10 Comparison between R and X evolutions of the five tests (calculated with offset = 0.0001)

5 Cyclical Evolution of the Discharge Slope

The evolution of the elastic modulus (Young's modulus) during fatigue test may be an indicator of material damage. We examine in the following the evolution of this parameter according to the number of cycles for the five specimens, his estimate is carried during the discharge on each hysteresis loop. A pseudo elastic modulus was determined by the slope of a regression straight line in a range of 40 % of maximum stress. Figure 11 shows the procedure for identifying of this pseudo elastic modulus. The evolution of the pseudo elastic modulus as a function of number of cycles is similar to the five tests. It can decompose in three phases, a fast decay of
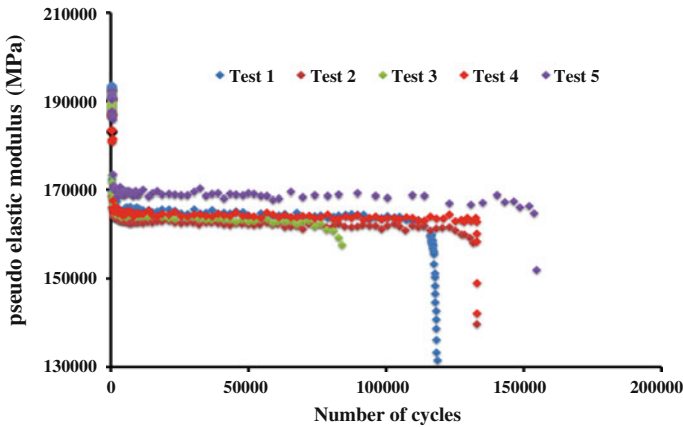
Fig. 11 Evolution of the pseudo elastic modulus during fatigue cycles for the five specimens

the pseudo elastic modulus is observed in the first cycles followed by a saturation phase and finally a new decrease phase. During the saturation phase, the calculated pseudo elastic moduli have a gap between them of the order of 2–3 % which is low.

6   Conclusions

The obtained results of performed fatigue tests at small controlled strain amplitude of 0.22 %, allows us to conclude that:

- The fatigue lifetime of the *304L* stainless steel varies from one specimen to another, even if they are loaded with a same manner;
- The evolution of the stress amplitude of the five specimens is unique. However, a small difference was found;
- The cyclic behavior of the *304L grade THYSSEN* is similar to this level of strain even if the frequencies of solicitation are different at the beginning of fatigue tests;
- The evolutions of *X* and *R* as a function of number of cycles show that these two components have a similar evolution during the fatigue cycles;
- The calculation of *R* taking into account a value of offset 10^{-4} does not render into consideration the behavior at the beginning of cycles for this steel with low applied strain amplitude;
- The evolution of the discharge slope is similar for the five specimens.

References

1. Taleb, L., Hauet, A.: Int. J. Plast. **25**(7), 1359–1385 (2009)
2. Vincent, L., Le Roux, J.C., Taheri, S.: Int. J. Fatigue **38**, 84–91 (2012)
3. Le Roux, J.C., Taheri, S., Sermage, J.P., Colin, J.F.A.: Pressure vessels and piping conference. Chicago, Illinois, USA (2008)
4. Taheri, S., Hauet, A., Taleb, L., Kpodekon, C.: Int. J. Plast **27**(12), 1981–2004 (2011)
5. Yoshida, F.: Int. J. Press. Vessels Pip. **44**(2), 207–223 (1990)
6. Colin, J., Fatemi, A., Taheri, S.: J. Eng. Mater. Technol. **132**(2), 021008–021013 (2010)
7. Colin, J., Fatemi, A., Taheri, S.: J. Mater. Sci. **46**(1), 145–154 (2011)
8. Cailletaud, G., Kaczmarek, H., Policella, H.: Mech. Mater. **3**(4), 333–347 (1984)
9. Belattar, A.: INSA de Rouen: Rouen, **185** (2013)
10. Kpodekon, C.: INSA de Rouen (2010)
11. Doquet, V. Taheri, S.: Revue Française de Mécanique, pp. 28–33 (2000)
12. Belattar, A., Taleb, L., Hauet, A., Taheri, S.: in Congrès Algérien de Mécanique. Guelma, Algérie (2011)
13. Dickson, J.I., Boutin, J., Handfield, L.: Mater. Sci. Eng. **64**(1), L7–L11 (1984)
14. Feaugas, X.: Acta Mater. **47**(13), 3617–3632 (1999)
15. Belattar, A.: Mécanique. INSA de Rouen, **185** (2013)